









Exploiting Spatiotemporal Properties for Efficient Event-Driven Human Pose Estimation

Haoxian Zhou , Chuanzhi Xu , Langyi Chen , Haodong Chen ,
Yuk Ying Chung , Qiang Qu , Xiaoming Chen , Weidong Cai 

Abstract—Human pose estimation focuses on predicting body keypoints to analyze human motion. Event cameras provide high temporal resolution and low latency, enabling robust estimation under challenging conditions. However, most existing methods convert event streams into dense event frames, which adds extra computation and sacrifices the high temporal resolution of the event signal. In this work, we aim to exploit the spatiotemporal properties of event streams based on point cloud-based framework, designed to enhance human pose estimation performance. We design Event Temporal Slicing Convolution module to capture short-term dependencies across event slices, and combine it with Event Slice Sequencing module for structured temporal modeling. We also apply edge enhancement in point cloud-based event representation to enhance spatial edge information under sparse event conditions to further improve performance. Experiments on the DHP19 dataset show our proposed method consistently improves performance across three representative point cloud backbones: PointNet, DGCNN, and Point Transformer.

Index Terms—Event camera, human pose estimation

I. INTRODUCTION

HUMAN Pose Estimation aims to predict keypoint positions from visual inputs to analyze body structure and motion. It has broad applications in action recognition, human-computer interaction, etc [1]. Deep learning has advanced RGB-based pose estimation [2], [3]. However, these methods remain challenged in low-light and high dynamic range scenes.

Event cameras are bio-inspired asynchronous sensors that capture per-pixel brightness changes at microsecond resolution. They provide high dynamic range, low latency, and sparse output [4]. These properties have enabled strong performance in motion deblurring [5], de-occlusion [6], depth estimation [7], HDR image reconstruction [8], 3D reconstruction [9] and super resolution [10]. Event cameras can overcome the limitations of frame-based cameras in extreme scenarios, enabling stable pose estimation.

Most event-driven human pose estimation methods rely on deep learning. Researchers have explored various event representations [11]–[13], such as event frames, to handle event sparsity as input to CNNs. Calabrese et al. introduced the first event-based human pose estimation dataset [14] with an event frame-based baseline method. Xu et al. combined event frames with grayscale images for 3D human motion

capture [15], but required heavy optimization. Later, Zou et al. estimated optical flow directly from events [16], which aimed to reduce grayscale dependence in [15]. Scarpellini et al. proposed the first monocular event camera approach for 3D pose estimation across three orthogonal planes [17]. More recently, some methods attempted to address the problem of pose disappearance in static scenes. Goyal et al. [18] introduced a novel event representation, Exponentially Reduced Ordinal Surface [19], to mitigate the temporal decay. Shao et al. [20] used a Long Short-Term Memory [21] network to recover missing information.

Most of the above approaches convert event streams into dense frames, which destroys sparsity and adds redundant computation. Furthermore, it is difficult to preserve dynamic temporal details for human pose estimation under such fixed frame-rate constraints. Only a few methods have exploited the sparse representation of events. Zou et al. converted event streams into spike-based representations [22] and employed spiking neural networks [23] to exploit event sparsity. However, this representation has limited capability to model the spatial geometric relationships of events. Chen et al. represented event streams as event point clouds and processed them with point cloud networks [24], achieving a balance between computational efficiency and spatial representation.

However, the point cloud-based method [24] overlooks the temporal properties of event streams. Since events are triggered by brightness changes, body parts that remain static do not generate events, making them unclear to be recognized. From our observation, this usually happens within short time windows, where neighboring slices contain essential motion cues. We believe that explicitly modeling temporal dependencies between adjacent slices can alleviate this issue.

Therefore, we propose a spatial edge-enhanced, point cloud-based network with explicit cross-slice temporal modeling. In particular, our method is further integrated into three different point cloud backbones, and experimental results show that our method achieves better performance than the original models.

Our contributions can be summarized as follows:

- We propose an Event Temporal Slicing Convolution (ETSC) module to capture short-term temporal dependencies across event slices, and integrate it into point cloud networks to fully exploit the sparsity and temporal features of event data for human pose estimation.
- We design an Event Slice Sequencing (ES-Seq) module that assigns event point clouds along the temporal dimension to provide temporally structured sequences.

Haoxian Zhou, Chuanzhi Xu, Langyi Chen, Haodong Chen, Yuk Ying Chung, Qiang Qu, and Weidong Cai are with the School of Computer Science, The University of Sydney, Sydney, NSW 2006, Australia (e-mail: chuanzhi.xu@sydney.edu.au).

Xiaoming Chen is with the School of Computer Science and Engineering, Beijing Technology and Business University, Beijing 100048, China (e-mail: xiaoming.chen@btbu.edu.cn).

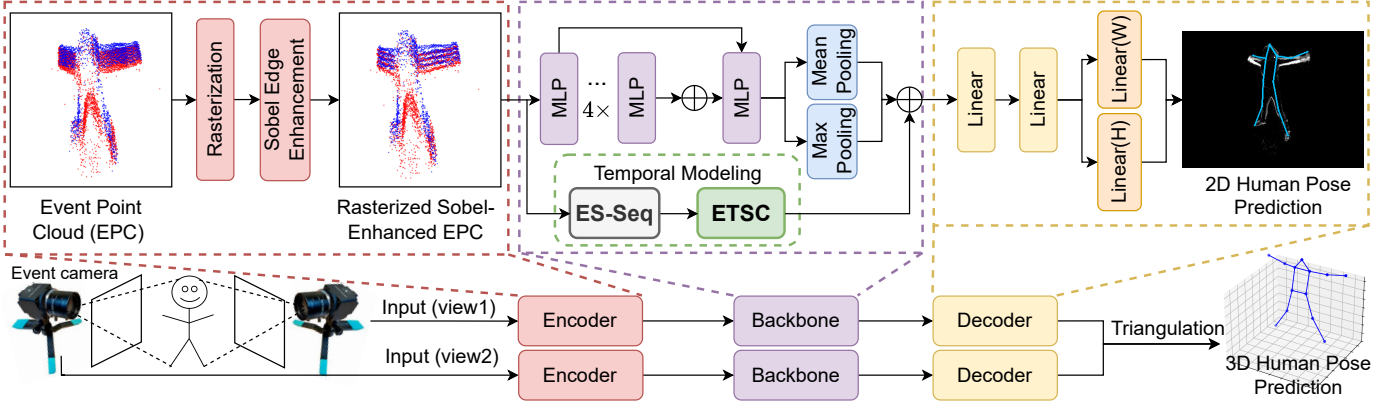


Fig. 1. Overview of the proposed pipeline. Event point clouds are rasterized with Sobel-based spatial edge enhancement and fed into the backbone. Temporal modeling with ES-Seq and ETSC refines the features, and SimDR [25] decodes 2D poses from each view, which are triangulated into the final 3D pose.

- We introduce an event Sobel edge enhancement module to strengthen spatial edge features in events and improve the model’s ability to perceive motion boundaries.

II. METHOD

Fig. 1 shows the overall pipeline of our proposed method, where we use PointNet serving as a representative backbone. To achieve 3D triangulation [14], at least two event cameras are required to capture the same object. The two cameras are placed at an oblique angle of approximately 90° to form a frontal binocular disparity. The dual-view input is then fed into the pipeline for processing. In the following, we describe our method in detail.

A. Rasterized Event Representation

An event camera produces an asynchronous and sparse event stream (x, y, t, p) , where (x, y) denotes the pixel coordinates, t is the microsecond-level timestamp, and p represents the brightness changes. We use the rasterized event point cloud representation proposed in [21] to leverage the sparse and spatiotemporal properties of events, instead of event frames.

Event cameras generate events at microsecond-level temporal resolution, and directly feeding all events into the network is computationally expensive. To reduce events while preserving information, we accumulate them on a pixel grid. Specifically, for a given time window $[T_i, T_{i+1})$, we divide it into K equal-length sub-segments. For each time slice, we aggregate events on a pixel grid. If multiple events $(t_m, p_m)_{m=1}^M$ fall into the same pixel (x, y) , we compute:

$$t_{\text{avg}} = \frac{1}{M} \sum_{m=1}^M t_m, \quad p_{\text{acc}} = \sum_{m=1}^M p_m, \quad e_{\text{cnt}} = M, \quad (1)$$

where t_{avg} denotes the average timestamp of events within the slice (normalized to $[0, 1]$), p_{acc} represents the accumulated polarity, and e_{cnt} denotes the event count. Finally, each valid pixel corresponds to a 5-dimensional point:

$$(x, y, t_{\text{avg}}, p_{\text{acc}}, e_{\text{cnt}}). \quad (2)$$

B. Spatial Edge-Enhanced Event Representation

Regarding spatial enhancement of events, Xu et al. [26] introduced a Sobel Event Frame representation to enhance spatial gradients for event-based 3D reconstruction. Following a similar motivation, we propose an event edge enhancement module that applies Sobel convolution in the voxel grid domain, making it compatible with the rasterized event point cloud representation.

Since events are triggered by brightness changes, the polarity p_{acc} directly reflects the sign of these changes, acting like a gradient direction signal. We aim to enhance p_{acc} to strengthen spatial edges and help the network better localize body parts under sparse event conditions.

First, we introduce an edge enhancement mechanism based on Sobel convolution in the voxel grid domain. Specifically, for each temporal slice, we construct an event count map $e_{\text{cnt}}(x, y)$ from accumulated events. We apply the classical Sobel operator to compute horizontal and vertical gradients:

$$G_x = \text{Conv2D}(e_{\text{cnt}}, K_x), \quad G_y = \text{Conv2D}(e_{\text{cnt}}, K_y), \quad (3)$$

where K_x and K_y are Sobel kernels. The edge magnitude is then obtained as:

$$E(x, y) = \sqrt{G_x(x, y)^2 + G_y(x, y)^2}. \quad (4)$$

Then, $E(x, y)$ is normalized by the maximum value within the same slice to ensure scale invariance across channels:

$$\tilde{E}(x, y) = \frac{E(x, y)}{\max E(x, y) + \varepsilon}, \quad (5)$$

where $\max E(x, y)$ indicates the maximum edge magnitude over the entire slice.

Next, we construct the enhancement weight:

$$w(x, y) = 1 + \alpha \cdot \tilde{E}(x, y), \quad (6)$$

where $\alpha \in [0, 1]$ controls the enhancement strength (set it at 0.5 in the experiment).

Finally, we perform per-pixel modulation on the selected statistic, the polarity accumulation p_{acc} :

$$p'_{\text{acc}} = w \cdot p_{\text{acc}}. \quad (7)$$

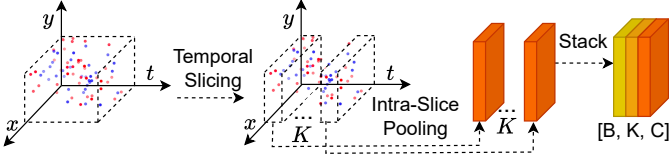


Fig. 2. Structure of the Event Slice Sequencing (ES-Seq) module.

The enhancement increases edge responses in the voxel grid stage, and the enhanced statistics are then exported as point cloud representations.

C. Temporal Modeling

To exploit the sparse structure of event point clouds for temporal modeling, we introduce the ES-Seq module as a novel representation that organizes unstructured event points into structured short-term temporal sequences, as shown in Fig. 2. First, the module maps each event point cloud into slices according to the normalized timestamp $t_{\text{avg}} \in [0, 1]$:

$$\text{slice_id} = \lfloor t_{\text{avg}} \cdot K \rfloor, \quad \text{slice_id} \in [0, K - 1], \quad (8)$$

where K is the number of temporal slices. In this way, each point is assigned to a fixed slice.

Within each slice, ES-Seq extracts point-level features from all points using max pooling to obtain a token representation:

$$t_{s,c} = \max_{n \in \text{slice } s} \text{feat}_{c,n}, \quad (9)$$

where s is the temporal slice index ($1-K$), c is the channel dimension, n is the point index within the slice, and feat is the point-wise feature representation of events.

Finally, the K slice tokens are stacked in temporal order to form a regularized short-term sequence:

$$\mathbf{T} = [t_1, t_2, \dots, t_K] \in \mathbb{R}^{B \times K \times C}. \quad (10)$$

Bai et al. [27] demonstrated the effectiveness of dilated 1D convolution for sequence modeling. However, their design mainly targets dense and long sequential data, which limits its applicability to event streams. In contrast, our proposed ETSC module operates on slice-level tokens rather than frame-level sequences and uses a dilated convolution and residual design optimized for ultrashort event sequences, enabling efficient short-term temporal modeling under sparse conditions. We feed the short-term sequence into ETSC to capture local motion patterns and temporal dependencies:

$$\mathbf{T}' = \text{ETSC}(\mathbf{T}), \quad \mathbf{T}' \in \mathbb{R}^{B \times K \times C}. \quad (11)$$

The structure of ETSC is shown in Fig. 3. Specifically, the module extracts local dependencies across slices using a standard convolution layer and a dilated convolution layer.

After obtaining the temporal token representations, we take the mean along the temporal dimension to obtain a global temporal vector:

$$t_{\text{global}} = \frac{1}{K} \sum_{i=1}^K t'_i \in \mathbb{R}^{B \times C}. \quad (12)$$

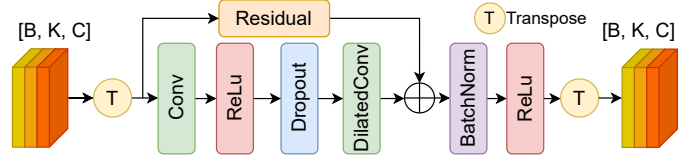


Fig. 3. Structure of the Event Temporal Slice Convolution (ETSC) module.

Then, we concatenate it with g_{max} and g_{avg} :

$$g_{\text{all}} = [g_{\text{max}}; g_{\text{avg}}; t_{\text{global}}] \in \mathbb{R}^{B \times 3C}, \quad (13)$$

where g_{max} and g_{avg} are obtained from feat by global max pooling and global average pooling over points.

As shown in the backbone of Fig. 1, we fuse temporal features with the pooled global maximum and average features to enable the model to exploit both temporal and spatial information, thereby enhancing feature representation.

III. EXPERIMENT

A. Datasets

DHP19 [14] is the only public event-based human pose estimation dataset that provides raw event streams, captured by four event cameras placed around the subject to provide 360° coverage, with 17 participants and 33 actions. The MMHPSD [16] was also captured using real event cameras, but it includes limited motion types and only publicly provides frame-based data. Therefore, we primarily use DHP19 in this work.

B. Implementation Details

We follow the existing work [14] by using subjects S1-S12 (training) and S13-S17 (testing). We adopt [24] as the main baseline, as it is the most relevant work using sparse event point clouds, while other methods differ in data representation and are not directly comparable. The number of temporal slices is set to $K = 4$, consistent with the rasterization process. All models are trained for 30 epochs using the Adam optimizer with a variable learning rate (1×10^{-4} initially, 1×10^{-5} after 15 epochs, and 1×10^{-6} after 20 epochs), a batch size of 32, and 2048 sampled points, on an RTX 5090 GPU.

We evaluate performance using Mean Per Joint Position Error (MPJPE), the average Euclidean distance between predicted and ground-truth joint positions in 2D (pixels) or 3D (millimeters), defined as:

$$\text{MPJPE} = \frac{1}{N \times J} \sum_{n=1}^N \sum_{j=1}^J \|\hat{\mathbf{p}}_{n,j} - \mathbf{p}_{n,j}\|_2, \quad (14)$$

where N is the number of samples, J the number of keypoints, $\hat{\mathbf{p}}_{n,j}$ the prediction, and $\mathbf{p}_{n,j}$ the ground truth.

C. Comparative Results

Table I shows our results, with \dagger indicating our reproduction, which shows similar results to the baseline. For 3D Event Point Cloud input, the baseline uses three different point cloud backbones (PointNet, DGCNN, and Point Transformer). We integrate our method into all three backbones, consistently

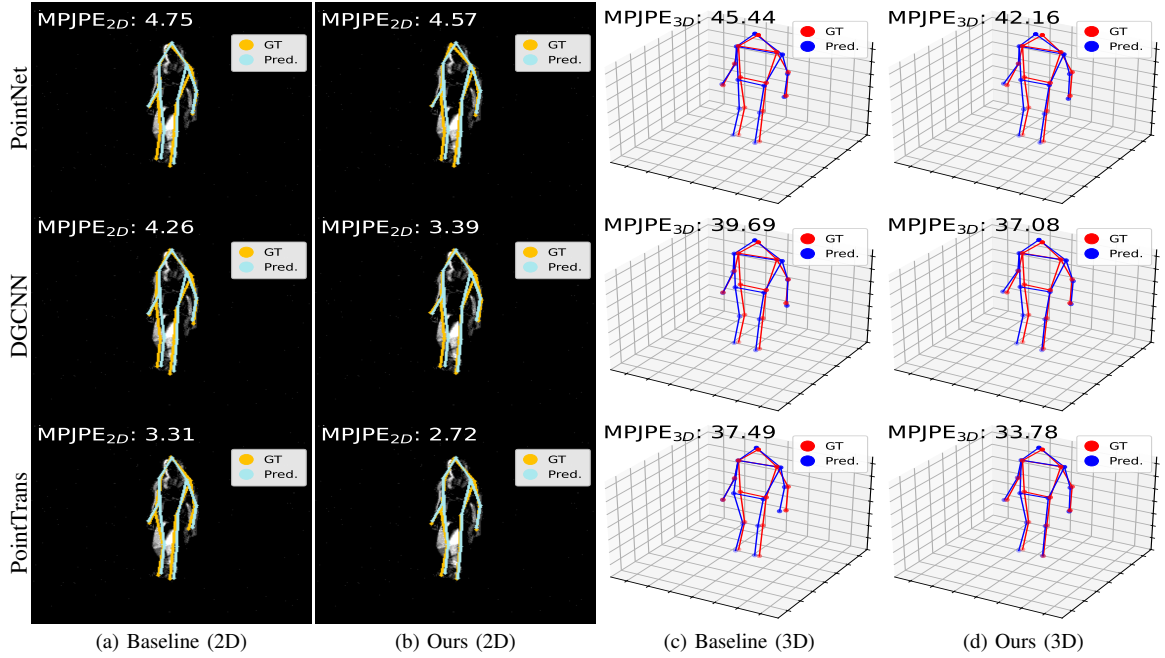


Fig. 4. Visualization of results from different models on the DHP19 dataset. (a–b) 2D results from cam3 view (baseline vs. ours). (c–d) 3D results via triangulation from cam2 & cam3 views (baseline vs. ours).

TABLE I
QUANTITATIVE RESULTS ON THE DHP19 DATASET.

Model	Method	MPJPE _{2D} ↓	MPJPE _{3D} ↓
PointNet	Baseline [24]	7.34	83.12
	Ours	7.09	80.16
DGCNN	Baseline [24]	6.85	77.68
	Ours	6.49	72.91
Point Transformer	Baseline [24]	6.57	74.30
	Ours	6.38	72.16

TABLE II
COMPLEXITY COMPARISON BETWEEN DIFFERENT INPUT TYPES.

Method	#Params (M)	#MACs (G)
Pose-ResNet18 [28]	15.4	8.30
Pose-ResNet50 [28]	34.0	12.91
PointNet (Ours)	8.65	1.18
DGCNN (Ours)	8.70	4.81
Point Transformer (Ours)	4.70	5.04

improving their performance: PointNet reduces 2D and 3D MPJPE by about 3.4% and 3.6%, DGCNN achieves the largest improvement (5.3% and 6.1%), and Point Transformer improves by roughly 2.9% in both metrics. Notably, our DGCNN surpasses the baseline Point Transformer while having a simpler architecture and lower computational cost. We also evaluated the real-time performance on samples of 7,500 events (about 0.13 s each) with a batch size of 1. PointNet and DGCNN achieve latencies of 1.89 ms and 3.73 ms, satisfying the requirement for real-time inference. Table II indicates the comparison of computational cost with frame-based methods, we follow the method [28], where the Pose-ResNet18 and Pose-ResNet50 models take a constant number (7500) of event frames as input. In contrast, our point cloud-based models use fewer parameters and MACs, effectively reducing computational complexity. Fig. 4 presents the visualization results. The

TABLE III
ABLATION STUDY ON THE PROPOSED METHODS.

Method	MPJPE _{2D} ↓	MPJPE _{3D} ↓
Baseline	7.34	83.12
Baseline + Temporal	7.12	80.56
Baseline + Temporal + Spatial	7.09	80.16

figure shows challenges such as leg motion blur and unclear edges in static regions where no events are triggered. Our method produces predictions that better match the ground-truth skeleton and achieves lower MPJPE than the baseline.

D. Ablation Study

We performed an ablation study on PointNet to test our modules. As shown in Table III, adding the temporal modeling module improves both 2D and 3D pose estimation, reducing MPJPE_{2D} and MPJPE_{3D} by 3.0% and 3.1%. This shows that modeling temporal dependencies helps capture richer spatiotemporal features and improves keypoint accuracy. Adding Spatial Sobel-based edge enhancement brings further improvements (about 0.4%), indicating that edge cues provide clearer structure to complement temporal modeling and enhance keypoint localization accuracy.

IV. CONCLUSION

In this paper, we propose an efficient event point cloud-based human pose estimation framework that integrates temporal modeling (ES-Seq and ETSC) with spatial Sobel-based edge enhancement. Our method achieves consistent improvement across multiple backbones, with the improved DGCNN even surpassing the baseline Point Transformer. In the future, we plan to explore more efficient spatiotemporal modeling for diverse event vision applications.

REFERENCES

- [1] T. B. Moeslund, A. Hilton, and V. Krüger, “A survey of advances in vision-based human motion capture and analysis,” *Computer vision and image understanding*, vol. 104, no. 2-3, pp. 90–126, 2006.
- [2] B. Xiao, H. Wu, and Y. Wei, “Simple baselines for human pose estimation and tracking,” in *Proceedings of the European conference on computer vision (ECCV)*, 2018, pp. 466–481.
- [3] Z. Cao, G. Hidalgo, T. Simon, S.-E. Wei, and Y. Sheikh, “Openpose: Realtime multi-person 2d pose estimation using part affinity fields,” *IEEE transactions on pattern analysis and machine intelligence*, vol. 43, no. 1, pp. 172–186, 2019.
- [4] G. Gallego, T. Delbrück, G. Orchard, C. Bartolozzi, B. Taba, A. Censi, S. Leutenegger, A. J. Davison, J. Conradt, K. Daniilidis *et al.*, “Event-based vision: A survey,” *IEEE transactions on pattern analysis and machine intelligence*, vol. 44, no. 1, pp. 154–180, 2020.
- [5] Y. Wang, C. Jiang, X. Jia, Y. Guo, and L. Yu, “Event-based shutter unrolling and motion deblurring in dynamic scenes,” *IEEE Signal Processing Letters*, vol. 31, pp. 1069–1073, 2024.
- [6] Y. Guo, W. Peng, Y. Chen, J. Zhou, and Z. Ma, “Improved event-based image de-occlusion,” *IEEE Signal Processing Letters*, 2024.
- [7] W. Chen, Y. Zhang, X. Sun, and F. Wu, “Event-based stereo depth estimation by temporal-spatial context learning,” *IEEE Signal Processing Letters*, vol. 31, pp. 1429–1433, 2024.
- [8] B. Ding, X. Yang, S. Yu, R. Dou, and L. Liu, “A fast hdr image reconstruction pipeline for hybrid event-frame camera,” *IEEE Signal Processing Letters*, 2025.
- [9] C. Xu, H. Zhou, L. Chen, H. Chen, Y. Zhou, V. Chung, Q. Qu, and W. Cai, “A survey of 3d reconstruction with event cameras,” *arXiv preprint arXiv:2505.08438*, 2025.
- [10] C. Xu, H. Zhou, L. Chen, Y. Y. Chung, and Q. Qu, “Ultralight polarity-split neuromorphic snn for event-stream super-resolution,” *arXiv preprint arXiv:2508.03244*, 2025.
- [11] A. I. Maqueda, A. Loquercio, G. Gallego, N. García, and D. Scaramuzza, “Event-based vision meets deep learning on steering prediction for self-driving cars,” in *Proceedings of the IEEE conference on computer vision and pattern recognition*, 2018, pp. 5419–5427.
- [12] A. Z. Zhu, L. Yuan, K. Chaney, and K. Daniilidis, “Ev-flownet: Self-supervised optical flow estimation for event-based cameras,” *arXiv preprint arXiv:1802.06898*, 2018.
- [13] D. Gehrig, A. Loquercio, K. G. Derpanis, and D. Scaramuzza, “End-to-end learning of representations for asynchronous event-based data,” in *Proceedings of the IEEE/CVF international conference on computer vision*, 2019, pp. 5633–5643.
- [14] E. Calabrese, G. Taverni, C. Awai Easthope, S. Skriabine, F. Corradi, L. Longinotti, K. Eng, and T. Delbruck, “Dhp19: Dynamic vision sensor 3d human pose dataset,” in *Proceedings of the IEEE/CVF conference on computer vision and pattern recognition workshops*, 2019, pp. 0–0.
- [15] L. Xu, W. Xu, V. Golyanik, M. Habermann, L. Fang, and C. Theobalt, “Eventcap: Monocular 3d capture of high-speed human motions using an event camera,” in *Proceedings of the IEEE/CVF Conference on Computer Vision and Pattern Recognition*, 2020, pp. 4968–4978.
- [16] S. Zou, C. Guo, X. Zuo, S. Wang, P. Wang, X. Hu, S. Chen, M. Gong, and L. Cheng, “Eventhpe: Event-based 3d human pose and shape estimation,” in *Proceedings of the IEEE/CVF International Conference on Computer Vision*, 2021, pp. 10996–11005.
- [17] G. Scarpellini, P. Morerio, and A. Del Bue, “Lifting monocular events to 3d human poses,” in *Proceedings of the IEEE/CVF Conference on Computer Vision and Pattern Recognition*, 2021, pp. 1358–1368.
- [18] G. Goyal, F. Di Pietro, N. Carissimi, A. Glover, and C. Bartolozzi, “Moveenet: Online high-frequency human pose estimation with an event camera,” in *Proceedings of the IEEE/CVF Conference on Computer Vision and Pattern Recognition*, 2023, pp. 4024–4033.
- [19] L. Gava, M. Monforte, C. Bartolozzi, and A. Glover, “How late is too late? a preliminary event-based latency evaluation,” in *2022 8th International Conference on Event-Based Control, Communication, and Signal Processing (EBCCSP)*. IEEE, 2022, pp. 1–4.
- [20] Z. Shao, X. Wang, W. Zhou, W. Wang, J. Yang, and Y. Li, “A temporal densely connected recurrent network for event-based human pose estimation,” *Pattern Recognition*, vol. 147, p. 110048, 2024.
- [21] A. Graves, “Long short-term memory,” *Supervised sequence labelling with recurrent neural networks*, pp. 37–45, 2012.
- [22] S. Zou, Y. Mu, W. Ji, Z.-A. Wang, X. Zuo, S. Wang, W. Si, and L. Cheng, “Highly efficient 3d human pose tracking from events with spiking spatiotemporal transformer,” *IEEE Transactions on Circuits and Systems for Video Technology*, 2025.
- [23] S. Ghosh-Dastidar and H. Adeli, “Spiking neural networks,” *International journal of neural systems*, vol. 19, no. 04, pp. 295–308, 2009.
- [24] J. Chen, H. Shi, Y. Ye, K. Yang, L. Sun, and K. Wang, “Efficient human pose estimation via 3d event point cloud,” in *2022 International Conference on 3D Vision (3DV)*. IEEE, 2022, pp. 1–10.
- [25] Y. Li, S. Yang, S. Zhang, Z. Wang, W. Yang, S.-T. Xia, and E. Zhou, “Is 2d heatmap representation even necessary for human pose estimation?” *CoRR*, 2021.
- [26] C. Xu, L. Chen, H. Chen, V. Chung, and Q. Qu, “Towards end-to-end neuromorphic voxel-based 3d object reconstruction without physical priors,” *arXiv preprint arXiv:2501.00741*, 2025.
- [27] S. Bai, J. Z. Kolter, and V. Koltun, “An empirical evaluation of generic convolutional and recurrent networks for sequence modeling,” *arXiv preprint arXiv:1803.01271*, 2018.
- [28] B. Xiao, H. Wu, and Y. Wei, “Simple baselines for human pose estimation and tracking,” in *Proceedings of the European conference on computer vision (ECCV)*, 2018, pp. 466–481.